## APPLIED RESEARCH

# Noncontact Detection of Cardiopulmonary Activities of Trapped Humans in Rescue Relief Events

**LINH PHAM**, (Member, IEEE), **MANORANJAN PAUL**, (Senior Member, IEEE), **AND PWC PRASAD**, (Senior Member, IEEE)
School of computing and Mathematics, Charles Sturt University, Bathurst, NSW 2795, Australia
Corresponding author: Linh Pham (lpham@csu.edu.au)

**ABSTRACT** Equipment for the correct identification of living objects entrapped under heavy debris is generally purpose-built, is costly, must be operated by highly trained professionals and is not readily available in a catastrophic event. A more readily available solution for improving the time-to-rescue ratio and logistics issues can be provided with smartphones which, equipped with software to find signs of life, are readily available at any disaster scene. This paper examines whether cardiac and pulmonary-related activities of living objects can provide acceptably accurate readings from a non-contact detection method. Laboratory experiments were conducted with Doppler radar at a 2.4 GHz frequency spectrum similar to smartphone-like devices, with empirical results demonstrating that human vital signs can be clearly identified when using smartphones for non-contact detection of living objects entrapped under debris. Experiments also simulated the psychogenic tremors likely to be experienced by individuals while operating the sensor-equipped devices under crisis conditions. The results show a clear relationship between the wavelength of pulmonary and blood vessel activities and the distance between the trapped human and the sensor in various conditions. The article also reports the design of a pseudo learning algorithm for model-based anomaly detection in time series to detect vital signs during normal and abnormal ventilation based on cardiopulmonary clinical records and datasets. This work significantly contributes to the existing body of research on timely rescue during disaster events.

## I. INTRODUCTION

Research into survival rates of disaster victims entrapped under rubble shows variations depending on whether or not the victim was injured, adequate fluid and sufficient space for movement of limbs were available, whether victims developed diarrhoea, the state of their overall health prior to the disaster, their age and how long it took to find them. A study compiled from 18 of 34 earthquakes highlights that rescue generally commences approximately 48 hours after the event, with the average time for detection and rescue being

The associate editor coordinating the review of this manuscript and approving it for publication was Alvis Fong.

6.8 days [1]. The longest time of entrapment of any victim ever found alive was 27 days [2] although this individual had access to dry food for the first few days. The latter is an exception rather than the norm, as international rescue organisations usually call off the search and rescue mission after 5 to 7 days, during which no further victims are found even if there are possible trapped victims who may be alive [3]. However, research opinions differ on the survival chances and the length of rescue commitment due to the many variations found in disaster events, Chiu *et al.* (2020), for example, argue that there is 74% survival chance if fully equipped rescue teams arrive within 24 hours, but diminish rapidly with every passing day.

Existing devices used for vital sign detection during rescue missions use mainly 22 or 40 MHz channel spaces at 2.4 GHz radio frequency spectrum, the wavelength is approximated to be 124.95 millimetres (mm). They carry a high cost, are time-consuming to deploy and generally require expert personnel to operate them. An example is the DKL LifeGuard [4] used after the earthquake in China in May 2008 [5] and during the World Trade Centre collapse in 2001. Similarly, the portable radar NASA FINDER was used to detect vital signs of victims trapped in the 2015 earthquake in Nepal [6]. Regarding frequencies used in non-invasive or contactless cardiopulmonary vital sign detection, significant research comes from Kara ([7], [8], who used 'line-of-sight' between the sensor and human subject. Lee *et al.* [8] and Girao *et al.* [9] deployed Microwave frequencies, while Kara and Sovlukov [10] experimented with Ultrasound. Less expensive systems have been proposed, such as the Doppler Radar sensor by Nosrati and Tavassolian [11] who operated at 2.4 GHz but only focused on the detection of passive intercostal muscle movement. At the same time, the subjects' chests faced the antennae, and there were obstacles (i.e., debris) between the live subject and the Doppler sensor. These research methods can all be used for detecting live objects trapped either less than a metre below the surface, using Ultra-wideband (UWB) [33] noncontact equipment or more expensive devices that are purpose-built with longer wavelengths and deeper penetration below the earth surface ([6], Baboli *et al.*, 2009; Barrie, 2015; [31])

However, all these systems have the same disadvantage: they need to be 'brought' into the disaster zone and are not readily available. What is required is a device that is commonly available that can be equipped to carry out the detection of vital signs of victims trapped under debris, such as smartphone-like technology. The number of these devices was reported to be above 6.5 billion globally at the beginning of 2022, and according to the United Nations, it is projected to shortly reach 7.8 billion [12]. There is, thus, a high probability of availability of smartphone-like devices when natural disasters occur in populated areas, enabling users to detect entrapped humans. The main objective of this paper is, thus, to introduce a robust, heuristic method for detecting live objects trapped under rubble achieved through reading vital signs using technology common to almost 7 billion individuals. To metamorphose the smartphone into an effective sensing unit, a Doppler sensor [13] at 2.4 GHz and pattern recognition and anomaly detection algorithm are proposed to deliver reliable sensing capabilities within one metre from the surface. It tends to simplify the calculation or resource crunch and maximise the device's battery longevity in crisis scenarios. Lab experiments to test the proposition were carried out using 0 to 60 seconds time-space sequences with results approximating 1000 mm for breathing (pulmonary) and 500 mm for near-skin vessel (vascular activities). The datasets were obtained from sensing signals from human bodies drawn from blood vessels under simulated conditions of entrapment (Fig. 1) [14], [15]. This work, thus, offers

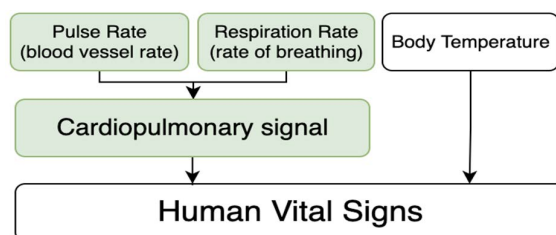a significant contribution to the timely rescue of trapped individuals in disaster events.



**FIGURE 1.** Essential vital signs of a living human subject.

A simple method was applied to identify the reflected radio signal from trapped subjects, either cardiopulmonary or pulmonary only and to estimate the distance between the human subject and the sensor. The human subject may be conscious or unconscious but hydrated if found immediately, the latter being likely to diminish after being trapped under debris for several days. If detection efforts commence soon after the event, still hydrated trapped victims will have more substantial blood flow and vital signs. Radio waves were compared in the laboratory while mimicking entrapment under the following materials: soil, brick, and concrete mix, as shown in Table. 1 configuration in the laboratory environment

To optimise short life of the battery, such smartphone-like devices and possible no grid power supply available during a crisis. A simple self-learning model-based anomaly detection in time series was then proposed to detect vital signs during normal and abnormal ventilation using a basic geometrical application of calculus based on the collected datasets from empirical research [16]. If the laboratory results from the setting of the Doppler radar sensor at 2.4 GHz RF spectrum generate a significant deviation from the trained mean, they are classified as anomalous [17]. For ease of operation, an embedded training module is proposed for training the anomaly algorithm.

Contributions of this paper are:
- Justification of the use of smartphones and tablet-like devices to detect vital signs from humans trapped under the rubble. Results of noncontact stationary and nonstationary or free movement of the Doppler sensor aimed at directions of interest which simulate actual conditions when holding actual smartphone-like devices to face down to suspect direction to detect the human subject configured as Fig. 4. (a), (b) and actual results of radio waves collected in a laboratory setup. This testing method aimed to find the acceptable noise threshold of radio wave propagation [11] and white and flicker noises [18] so that the reflected signal is still recognisable. A pre-defined anomaly vital signs algorithm can learn it.
- Proposal for a non-situated sensor capable of hovering above a surface and moving within 10 degrees to trail for pulmonary hotspots on the human body. A non-stationary sensor can float freely within a pre-defined range and capture groin, wrist, ankle, and cardiac neck

activity. Thus, widening the chance of detection of survivors of a disaster event.

- Recognition of the importance of pulmonary hotspots on the human body. These points have not so far attracted significant attention. As they are distributed across different regions of the human body, it is only in conjunction with the non-stationary sensor that they may be found with more ease.
- Design of the theoretical model for a self-learning algorithm to detect abnormalities in cardiopulmonary activities. The efficacy of this heuristic method lies in its ability to validate the previously published observable wavelet dataset for a human subject trapped under debris relying on noncontact (i.e., non-invasive) vital sign sensors for the correlation between heart rate and breathing beat activities.

The remainder of this paper is arranged as follows: The laboratory setting, hardware, Doppler radar sensors and noncontact data collection methods are presented in Section II followed by the results of the blood vessel and breathing activities in MATLAB (Section III). Section IV proposes and plots simple model-based anomaly detection in time series. The conclusion and further perspectives are given in Sections V and VI with conflict of interest and funding declaration, data collection on human compliance ethical standards and acknowledgement found at the end of the paper.

## II. CARDIOPULMONARY SIGNAL READING METHODS

This section describes the technology behind the Doppler Effect radar technique and the laboratory Doppler sensor configuration used in this research to send wavelengths through obstacles and collect vital signs signals. The elements of interest in living human body regions were blood vessels and breathing activities. Participants are also identified and briefly described together with the terms of the ethics approval terms.

### A. DOPPLER EFFECT RADAR TECHNIQUE

The concept of contactless vital sign detection and monitoring using microwave has been applied since the 1970s [19] primarily for non-invasive, non-intrusive and unobtrusive medical diagnosis, including monitoring of foetal heartbeat, air emboli, blood pressure and blood flow [9]. In the context of a short theoretical study related to stellar motion, Christian Johann Doppler, using a simple formula, demonstrated the deviation of sin waves [20]. Doppler radar technologies have been widely used in many applications, such as vehicle speed measurements, automotive obstacle detection, and storm tracking and mapping [18]. More recently, these technologies have also been applied in the medical domain, in areas such as medical imaging and heart rate and pulmonary monitoring [9]. A significant body of research and experiment apply Doppler Effect radar techniques in a broader range of radiofrequency spectrums and bands. They started at 450 MHz or 1500 MHz to detect vital signs through earthquake rubble and concrete approximate 3 meters thick [21], to $K_a$ band from 20-30 GHz.

JalaliBidgoli and colleagues have successfully tested and collected vital signs of human subjects 1.5 to 10 meters below the surface subject to material density with a Doppler effect sensor operated at 1.15 GHz and equipped with two horn antennae [22]. Countless architectures for signal compensation and filtering noise techniques have been proposed and tested within these RF ranges [18], [19]. The advantage of the Doppler Effect and the prior knowledge of vital sign signals has provided massive scope for applying Doppler Effect radar with a similar RF range at 2.4 GHz RF range.

The Doppler radar receives the reflected signal through the receiver antenna, while radar outputs are through in-phase (I) and quadrature-phase (Q) signals (channels) [11]. Fig. 2 represents how the elastic movement generated by the human subject is collected by two configured transmit (Tx) and receiver (Rx) antennae.
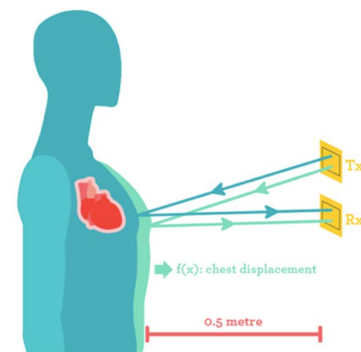


**FIGURE 2.** A sample of how Doppler radar detects the chest wall elastic movement by directional antennae.

### B. HARDWARE SETTINGS

Our laboratory experiment was comprised of the Doppler sensor configuration and used standardised 2.4GHz Industry Science and Medical (ISM) frequency ranges [23]. The Doppler sensor antennae circuit emits a single-tone signal obtained from Year One LLC, as given in Fig. 3, to detect the contractions of human subjects' near-skin vessels and the respiratory muscles and measure the elasticity of the movement. The readings of vascular and breathing activities are in the form of voltage changing as amplitude in 60 seconds, converted to Microsoft Excel format as the final dataset ready for analysis and plotting. The setup includes a 2.4 GHz Doppler radar circuit board, two patch antennae, a four channel-equipped DATAQ Model DI-1100 data acquisitor and a four AAA battery box or 6-DC voltage.

### C. VITAL SIGNS SENSING METHODS

To support the empirical research goals of the article, we only focus on collecting human subjects near-skin vessel and torso displacement activities. After a number of radio wave reading methods have been carried out over the research duration, we identify two methods that can be used to maximise the ability to detect whether there is a possible sign of human object entrapment under rubble during a period of fewer than 60 seconds. These two reading methods are tested when
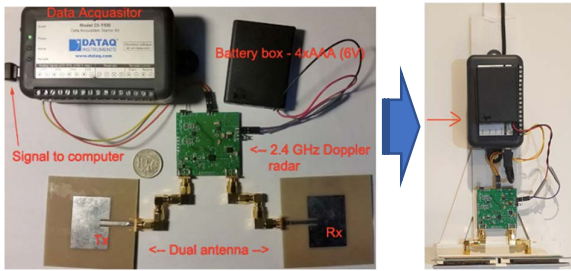
**FIGURE 3.** Doppler sensor components are mounted on a wooden stick, making it easier to maneuver and create random variation datasets rather than placing the sensor on the actual surface.
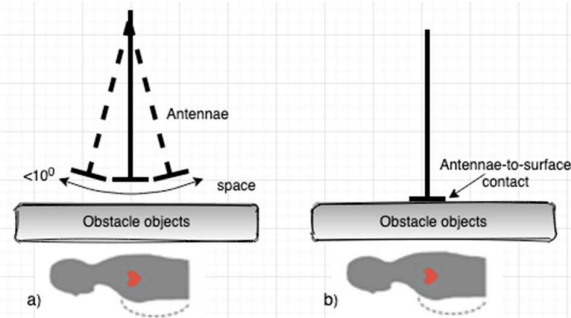


**FIGURE 4.** a) Doppler sensor is move-free in any direction and not contact the surface. b) Regular antennae-to-surface contact configuration when collecting radio wave.

**TABLE 1.** Brick, Soil, and Concrete-mix materials used in radio wave propagation comparison results.



| a) Brick | b) Soil | c) Concrete Mix | d) Soil - Brick | e) Concrete Mix - Soil - Brick |
|---|---|---|---|---|

the sensor positions are in 'contact' with the rubble surface (b) and 'non-contacted' or randomised (a) with an agreed angle and dimensions, as illustrated in Fig. 4.

The first method is to detect and validate the collected signal against the trained vascular label, as shown in Table 2, to see whether or not periodic vascular activities can be identified in a human subject.

Based on the research scope mentioned above, we aim for the near-skin vessel regions shown in Fig. 5. This experiment will not investigate deeper closed-blood vessel systems beneath the skin such as major arteries and veins [24] that are usually analysed by human subject with touch-based ultrasound techniques for blood flowmeter or scanner [25], [26] or the traditional medical contact-based physiological monitor devices.

The second method is to collect radio waves and challenge pre-trained pulmonary labels (Table 3) for a human subject's breathing activities or torso's nonstop displacement as if the subject were still alive. Positions of human subjects during real disaster scenarios may be far more varied. Therefore, multiple positions and angles to the sensor antennae were
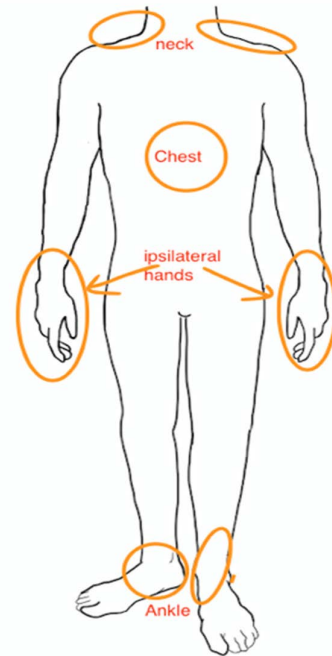


**FIGURE 5.** Detectable blood vessel activities and regions using noncontact Doppler sensors for living subjects.

designed, and the human subjects were positioned in the laboratory so that a range of variations could be reflected in a dataset. The assumption is that the estimated object position is unknown to the sensor when a human subject is trapped under rubble and not visible to the naked eye. Thus, a breathing dataset from four different angles was collected as samples presented in this paper, and each position was rotated by 90-degree, as shown in Fig. 6.
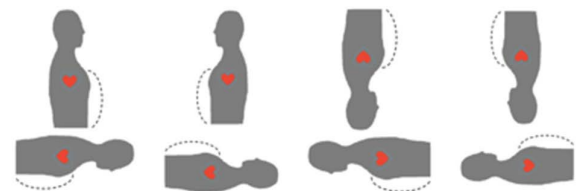


**FIGURE 6.** Difference of victim position samples in rescue relief events.

### D. PARTICIPANTS INFORMATION

Participants in the laboratory environment were volunteers who had read the information sheet and signed the consent form as per the terms and conditions of the ethics approval for this research project. Ethics approval was obtained with approved protocol number 200201755 for research involving human participants; refer to compliance with ethical standards at the end of the paper for details.

### III. CARDIOPULMONARY RESULTS AND ANALYSIS

The actual laboratory dataset results and wave signal plotted below were produced from the regular and irregular activities of human subjects' artery vascular system and strong artery near-skin regions. The diaphragm's contraction and

**TABLE 2.** Acceptable ranges of heart rates [27] and labelled as contacted or pre-trained heart rate or beat in this paper.

| Age group | Beat per 60 seconds | Beat per 30 seconds |
|---|---|---|
| Infants | 120-160 | 60-80 |
| Toddlers | 90-140 | 45-70 |
| Pre-schoolers | 80-110 | 40-55 |
| School-agers | 75-100 | 37-50 |
| Adolescent | 60-90 | 30-90 |
| Adults | 60-100 | 30-50 |

**TABLE 3.** Acceptable ranges of respiration rates [30] and labelled as contacted or pre-trained respiration or pulmonary in this paper.

| Age group | Rate per 60 seconds | Rate per 30 seconds |
|---|---|---|
| Newborns | 30-60 | 15-30 |
| Infants | 30-50 | 15-25 |
| Toddlers | 25-32 | 12-16 |
| Child | 20-30 | 10-15 |
| Adolescent | 16-19 | 8-10 |
| Adults | 12-20 | 6-10 |

relaxation are shown when the 2.4 GHz Doppler sensor is contacted and situated on the top of the surface, as in Fig. 7 and when moving randomly over the surface of interest, as in Fig. 15. Thus, this paper aims to detect the possible inverted wave signal from entrapped subjects of interest not visible to the naked human eyes.

Once the reader collects the wave signals, the next phase is to compare these against the predefined cardiopulmonary labels and show whether there is any possible match with the human heartbeat and breathing rates listed in Tables 2 and 3 (collected by traditional contact instruments such as electro-cardiography for heart rate and impedance pneumography or capnography methods for breathing rate collections) [27]. For a more manageable comparison for the remainder of this paper, we labelled heart and respiration rate datasets in these two tables as contacted or trained heart rate or beat and respiration or pulmonary rate, respectively.

In comparison, dog and cat heart rates are approximately 70-220 and 120-240 beats per minute [28] respectively, while dogs' breathing rate is 15-30, and cats 15-40 breaths per minute when at rest [29]. As the research focuses on human subjects' vital signs, we did not obtain ethical approval to work and experiment with animals. However, the method implied in this paper could detect any living subject with suitable inverted cardiopulmonary wave rhythm reflected from regions of interest.

Heartbeat and Living humans' heartbeat rate patterns of living human age, activity, illness, and emotion are affected by drugs [27], [30]. In scenarios of subject entrapment, there are additional factors such as temperature conditions, different degrees of injury, emotional stress, anxiety, fear, hunger, etc., to be considered when projecting and accessing the subject's state. However, the goal of this study is to detect any sign of a living subject beneath the surface of debris and display the results in the shortest possible time. Here,

the analysis from both vessel system and respiration signals employed quick detection at 30 and 60 seconds intervals.
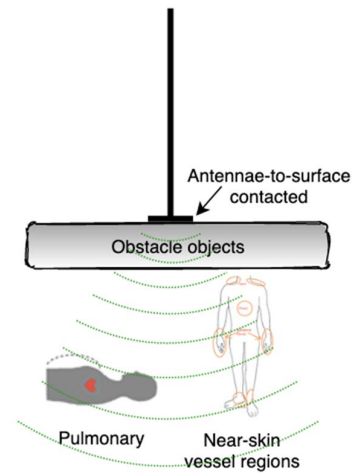


**FIGURE 7.** Sample of Doppler sensor's antennae situated on the top and in contact with the surface when reading vital sign.

## A. ANTENNAE CONTACTED THE SURFACE
### 1) PULMONARY RESULTS

The samples for the breathing dataset were collected in this experiment from two patch antennae penetrating through 50 mm solid building grade bricks placed on top of a 5 mm thick wooden board and a 2 mm wooden board, as in Fig. 9, mimicking physical entrapment of a human subject under building materials. Participants were instructed to breathe normally within 0 to 30 seconds and abnormally within 30 to 60-second intervals to generate a variety of datasets for one minute. We further simulated a rescue relief operation to detect the breathing across four different positions of a human subject as shown in Fig. 8, a), b), c), and d), the naming convention is listed in Table 4. C2A - chest to antennae – was simulated with Fig. 2, where Tx and Rx are directional antennae for transmission and reception.

Following is a random dataset representative of six participants at four different estimates of 90-degree angles and the position of the torso to antennae to detect the displacement of the intercoastal muscles generated when in- and exhaling. Each result illustrates a plot to virtualise the vital sign graphically ranging from 0 to 30 seconds. Fig. 10 accounts for normal breathing, while the abnormal breathing is displayed in Fig. 10, which calculates the mean of all collected outliers and skewed points and projects the results in a scatter plot allowing comparison with the respiration rates per 30 seconds in Tables 6 and 7. For example, human subject (HS) participant 1 was in a resting state. Five respiration-related displacements were detected with chest faced to antennae (C2A) position or 0° angles as pre-labelled in Table 4.

In this laboratory-based pulmonary signal reading sample, human subjects were positioned at four different 90-degree angles to the stationary Doppler antennae right above the subject to create positional datasets, as in Tables 5. and 6.

**TABLE 4.** Positions convert to a degree for plotting purposes.

| | |
|---|---|
| $0^0$ as C2A | The human chest wall faces the sensor antennae, and the human back is on the floor |
| $90^0$ as R2A | The human right side faces the sensor antennae, and the left side is on the floor |
| $180^0$ as B2A | The human back faces the sensor antennae, and the chest wall is on the floor |
| $270^0$ as L2A | The human left side faces the sensor antennae, and the right side is on the floor |



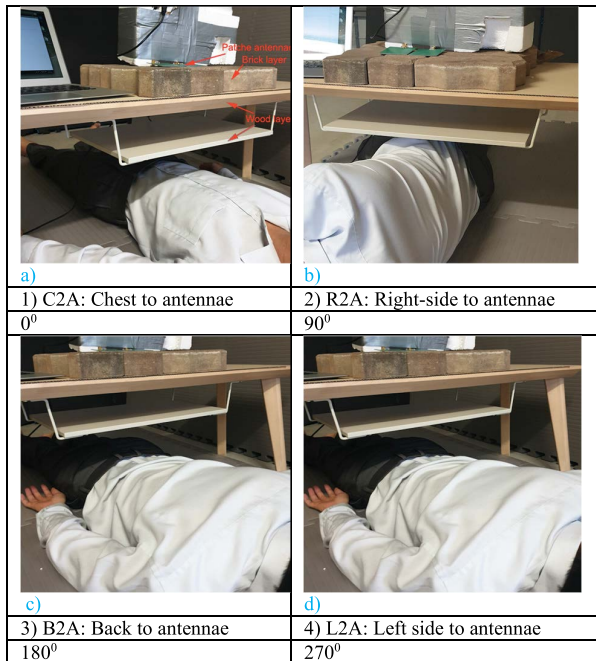| a) | b) |
|---|---|
| 1) C2A: Chest to antennae $0^0$ | 2) R2A: Right-side to antennae $90^0$ |
| c) | d) |
| 3) B2A: Back to antennae $180^0$ | 4) L2A: Left side to antennae $270^0$ |

**FIGURE 8.** Participant position samples aim at the torso for breathing signal.

**TABLE 5.** Doppler sensor collected 0 to 30 seconds – Normal or at resting breathing for a human subject (HS).

| Angle of Doppler | HS1 | HS2 | HS3 | HS4 | HS5 | HS6 |
|---|---|---|---|---|---|---|
| $0^0$ | 5 | 7 | 6 | 7 | 8 | 8 |
| $90^0$ | 5 | 8 | 5 | 7 | 10 | 10 |
| $180^0$ | 7 | 7 | 6 | 8 | 9 | 9 |
| $270^0$ | 5 | 9 | 6 | 6 | 8 | 8 |

The normal breathing rate plotted in Fig. 9 is between 0 to 30-second intervals. Data in Fig. 10 reflects deeper in- and exhalation by participants to simulate abnormal breathing, reading the results for approximately 30-60 seconds. Noting that the differences in the level of direct current (DC) voltage vertical axis are due to the distance between the human subject and the patch Tx for transmission and Rx for the receiving antennae, the actual voltage input is positive. If the human subject is closer to the sensor, output power consumption falls but increases with greater distance. File-name.xlsx is a Microsoft Excel file format converting voltage changes for 60 seconds of input from the Doppler reader. To trace multiple datasets more efficiently for each participant across four different positions, the naming convention was used. For instance, S1.R2A.xlsx is labelled for the first

**TABLE 6.** Doppler sensor collected 30 to 60 seconds – of deep abnormal breathing.

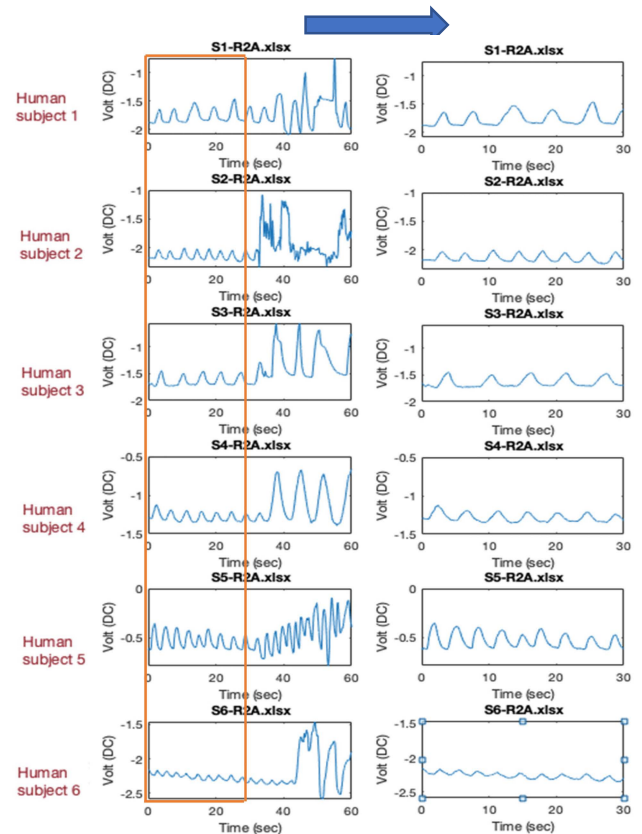| Angle of Doppler | HS1 | HS2 | HS3 | HS4 | HS5 | HS6 |
|---|---|---|---|---|---|---|
| $0^0$ | 5.5 | 7 | 6 | 5 | 6 | 5.5 |
| $90^0$ | 7 | 7 | 5 | 5 | 13 | 7 |
| $180^0$ | 6 | 9 | 6 | 7 | 7 | 9 |
| $270^0$ | 6 | 8 | 6 | 5 | 7.5 | 8.5 |



**FIGURE 9.** 90° (R2A) of six participants plot in 0-30 seconds normal ventilation or at rest breathing.

participant right side faces the sensor antennae, and the left side is on the floor, as named in Table 4 and illustrated in Fig. 9.

The population mean (1) was used to calculate the complete data set recorded in Tables. 5 and 6 for 0 to 30 and 30 to 60-second intervals to produce complex datasets and results.

$$\mu = \frac{1}{N} \sum_{r=1}^{N} HS_r \quad (1)$$

where,

$\mu$ = population mean
$N$ = size of the population
$\Sigma$ = the total of all sample
$HS_r$ = respiration samples collected
Apply (1) to the Table. 5 dataset and result as (2)

$$\mu_{0-30 \text{ sec}} = \frac{1}{24} \sum_{r=1}^{24} (24 \text{ results in Table 5}) = 7.08 \quad (2)$$
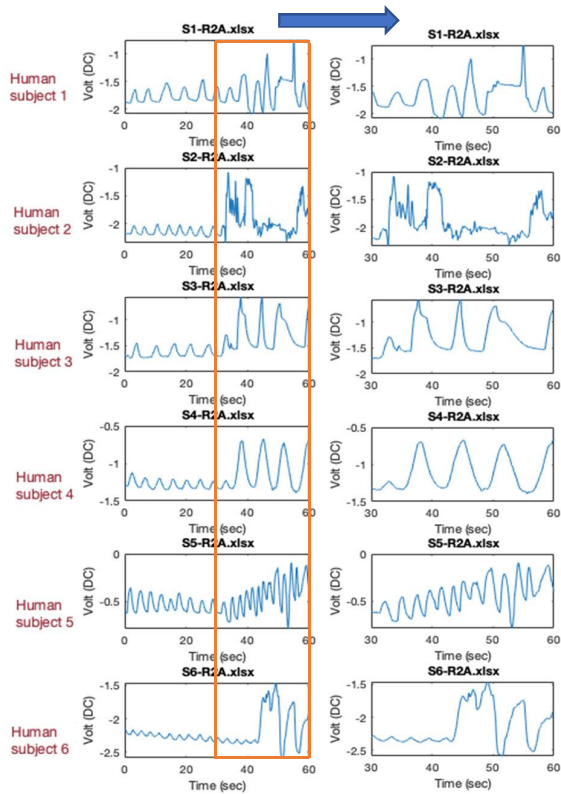
**FIGURE 10.** 90° (R2A) of six participants plot in 30-60 seconds with intended deep abnormal breathing than first 30 seconds.



**FIGURE 11.** Population mean of normal breathing result of six time series collected when sensor contact with the surface.



**FIGURE 12.** Population mean of abnormal breathing result of six time series collected when sensor contact with the surface.

Figs. 12 and 13 show that the population means are the same regardless of angle or human subject. The population mean $\mu$ is the same in both methods and falls into the standard contact respiratory monitor from 0 to 30 seconds. The result is $6 \leq \mu_{0-30} \leq 9$, which matches the standard clinical data for an adult's breathing rate movements during a 0 to 30 second period.

Apply (1) to the Table 6 dataset and result as (3)

$$\mu_{30-60 \text{ sec}} = \frac{1}{24} \sum_{r=1}^{24} (24 \text{ results in Table 6}) = 6.98 \quad (3)$$

When producing abnormal readings, participants were instructed to make random moves with their hands and legs and take deep and sharp breaths for both in- and exhalation in the trapped position, as shown in Fig. 10 during the 30-60 seconds.

However, the results remained the same. The estimated population mean resulting from (2) and (3) also fell within the standard invasive respiration range for an adult, $6 \leq \mu_{30-60} \leq 9$. In contrast to the actual clinical dataset from Table 3 [30] for acceptable ranges of respiration rates, the collected result falls well within the adult breathing rate for a 30-second duration. According to Figs 11 and 12, the Y-axis represents the breathing rate, and the X-axis the six readings across four different positions. It is noted that standard breathing patterns can vary with age, activity, illness, emotions, depressive thoughts, drugs, and state of amusement.
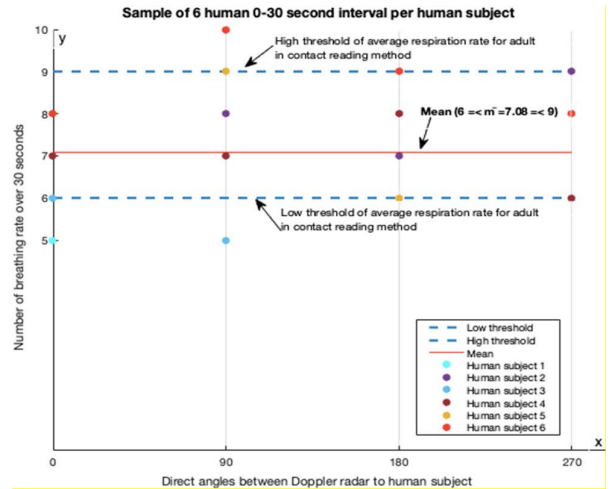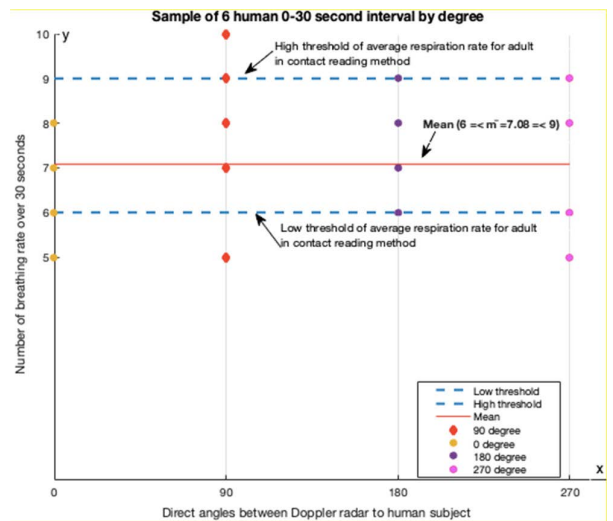
To simulate the complexity of behaviours of trapped objects, a variety of outputs was produced with results shown in Fig. 9, with all participants breathing normally and did not move for 0 to 30 seconds. Fig. 10 reflects that the participants had been instructed to move their body parts slightly, including hands and legs. The respiration results fell between adults' standard invasive respiration range, Table 3 in 30 seconds, $6 \leq \mu_{0-30}$ or $\mu_{30-60} \leq 9$ regardless of the object's position and the angles at which the Doppler radar antennae was face.

**2) VASCULAR OR NEAR-SKIN VESSEL RESULTS**

Fig. 8 shows sample positions with a distance of fewer than 0.5 metres from the Doppler sensor and the nearest vascular populated region (Fig. 5); hands were used in this case. The sensor is in contact with the surface (Fig. 7), and blood vessel-related signals are collected. Three samples plotted as Figs. 13, 14 and 15 are based on 5 seconds of sensing
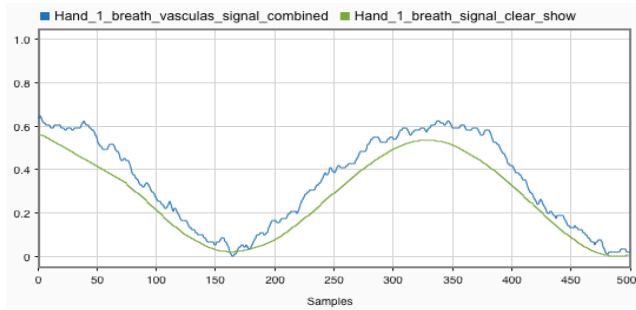
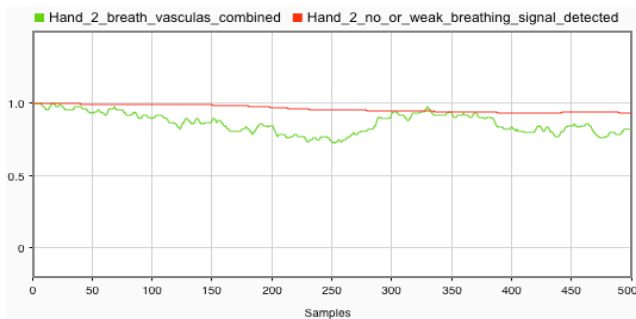**FIGURE 13.** Hand area 1 - both near-skin vascular and breathing signals coexist.



**FIGURE 14.** Hand area 2- mainly near-skin vascular, and no significant breathing signal detected.
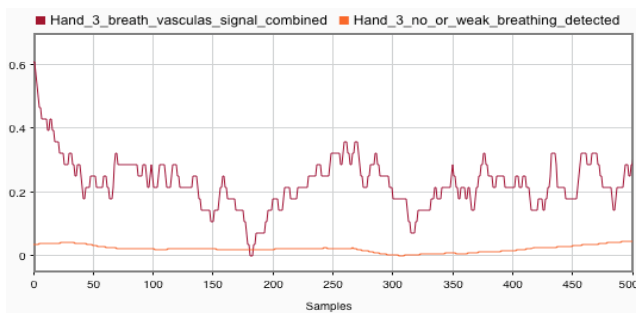


**FIGURE 15.** Hand area 3 - mainly near-skin vascular, and no significant breathing signal detected.



**FIGURE 16.** Doppler sensor randomly moving on the top of the earth's surface sample.



**FIGURE 17.** Actual simulation of Fig. 16. configuration when sensing radio wave while Doppler radar move randomly in any direction.

operation and 500 samples collected from the hand/palm areas while the Doppler sensor antennae had contact with the surface during the reading of the vital signs.

Discussion part V contains the analogy result between the stationary and mobile Doppler sensor (i.e., not touching the obstacle surface). The contrast for both near-skin vascular detection methods and breathing signals indicated that the objects of interest were less than 0.5 metres from the Doppler sensor. Aligned with the vital sign detection study in this paper, the three experiments above test whether there are differences in blood-related vessels and activities between the sensor that touches and does not touch the surface and whether both methods provide a sign of life signal. With the current hardware setting used in the paper, no blood vessels or near-skin displacement activities were detected
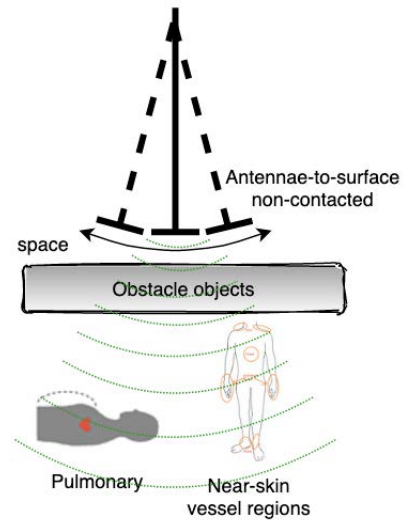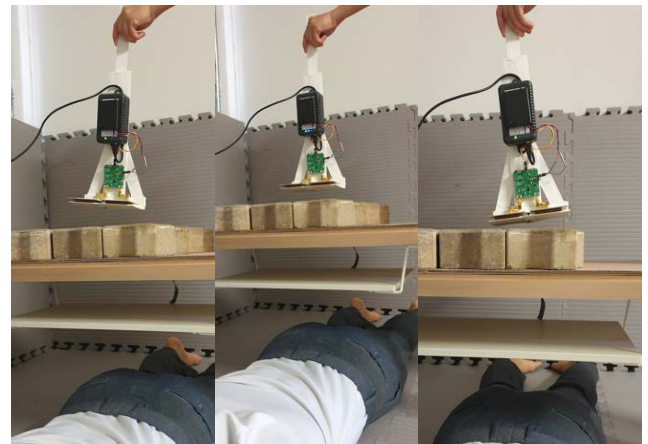
if the object exceeded 0.5 meters in the distance from the antennae.

### B. ANTENNAE RANDOM MOVEMENT ON THE SURFACE

Most recent empirical research into noncontact detection of vital sign cardiopulmonary-related signals has been conducted with sensors firmly in contact with the obstacle surface [31]–[33]. The purpose of this data collection design is to create a variety of datasets with the same duration to identify if there are significant outliers and variations in one time series from a collection of time series when the Doppler sensor antennae are in contact with the surface of interest (Fig. 7) or mobile and not in contact (Fig. 16). Here, instead of locating the Doppler radar so that it touches the surface of interest, the data collection design allows free movement to the Doppler antenna within 5-10 degrees from a fixed point above the surface of interest. Results were plotted in Figs. 18 and 19 for the pulmonary and near-skin vessel.

### 1) PULMONARY RESULTS

Fig.16 simulates free sensor movement above the target of interest until the input wave is no longer recognisable and identifiable by the pre-defined cardiopulmonary algorithm compared to clinical threshold values from Tables 2 and 3. Fig. 18 plotted different datasets for three different positions and Fig. 17 for 30 seconds of time-space. The signal analyser shows only pulmonary and no near-skin vessel signals co-existing, see Fig. 13.
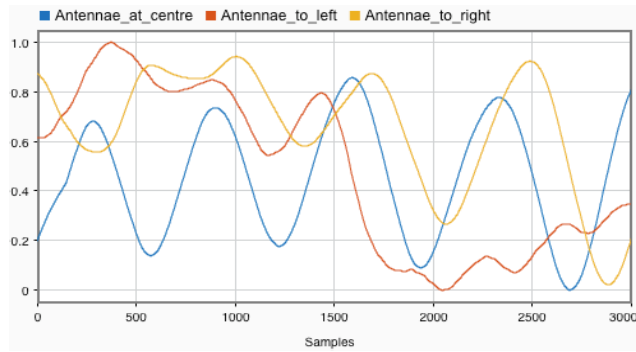


**FIGURE 18.** Plots collected datasets from Figure 17 sample positions where the sensors were moved around from the center point.

Fig. 18 shows the Doppler being subjected to shaking possibly caused by nervousness, also producing a slight deviation from the centre-point by less than 10 degrees with the object being no more than 1 meter in the distance. The breathing signal is still recognisable. The experiment recorded that when the angle of the random movement was approximately 10 degrees, the reflection of the breathing wavelength reading was getting weaker and eventually disappeared completely.

### 2) VASCULAR OR NEAR-SKIN VESSEL RESULTS

Similar manoeuvres and settings were used for pulmonary signal collection for a non-stationary sensor above the surface (Figs. 17, 18). The comparison was drawn between results of the near-skin vessel when the sensor was in contact and freely moved above the detection area of interest. Fig. 19 projected results from 5 seconds of sensing operation and 500 samples and aligned with (Figs. 13, 14 and 15) the near-skin vessel when the sensor was in contact with the surface during data collection.
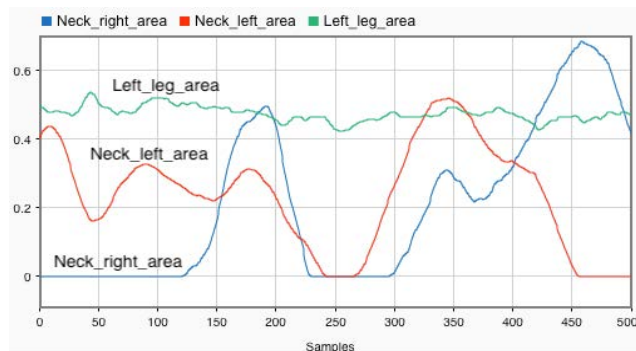


**FIGURE 19.** Near skin-vessel detection when a sensor is freely movement on the top of the neck, leg areas.

Fig. 19 shows no sign of near-skin vessel or vascular wavelength being detected on the left and right neck areas, but pulmonary activities appeared strongly from the reading result. The Doppler sensor indicated the blood-related vessel but detected no displacements caused by breathing from the leg region.
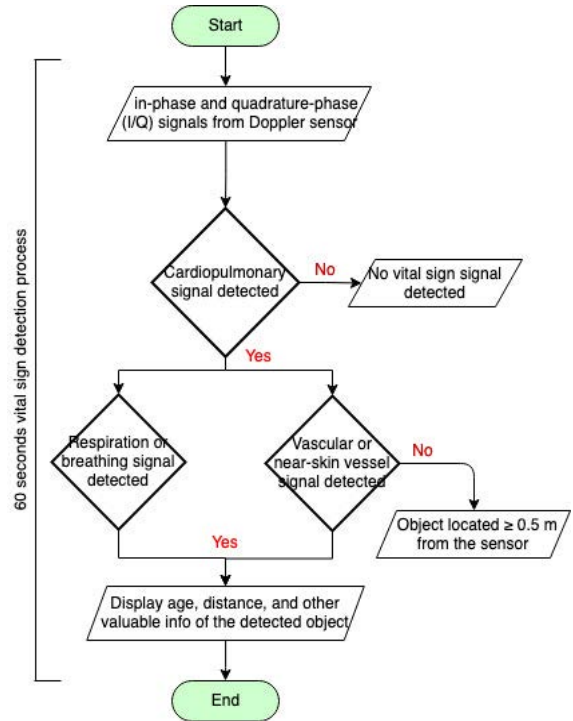


**FIGURE 20.** Flowchart of the proposed cardiopulmonary noncontact detection in 60 seconds interval.

## IV. PROPOSED ANOMALY ALGORITHM USE IN CARDIOPULMONARY NONCONTACT DETECTION

In this section, we proposed a learning anomaly detection algorithm based on the collected dataset from empirical [16] laboratory results [16] produced from the setting of a Doppler radar sensor at 2.4 GHz RF spectrum explained in Section III – Cardiopulmonary results showed a significant deviation from the trained mean, Figs. 11 and 12 have been classified anomalous [17]. In a scenario where humans are trapped under debris during disaster events, it is likely that potential rescuers on the surface would experience states of high anxiety, which may cause their hands to shake and cause tremors to the small palm-size device, likely to increase with the lengths of sensing time. Hence, a shorter time in holding still such a device would be logical and also lead to better device battery utilisation. We used 30- and 60-second timespans to collect, observe, and plot the vital sign signals throughout the project. The same time-series strategy was also reemployed in the algorithm. The main objectives to be addressed from this learning anomaly detection algorithm include:

- Phase I: From 0 to 30 seconds, establish whether there are any likely signs of living objects entrapped under rubble.

**TABLE 7.** Model-based anomaly detection in time series proposed algorithm: model-based anomaly detection in time series.

**Algorithm:** Model-based Anomaly Detection in Time Series
**Input:** Noncontact breathing and near-skin vessel In-Phase and Quadrature (I/Q) signal sensed from Doppler radar for 60 seconds duration
**Output:** Pulmonary signal only or both blood-related pulse and pulmonary signal found, and possible health status indications or no vital sign signal found in 60 seconds time-space.

The total number of high and or low outlier deviations can be expressed as
$$\$result = \sum_0^{30}\{f'(x) = 0, f'(x) < 0\} \cup \sum_0^{30}\{f'(x) > 0, f'(x) = 0\} \qquad (3)$$
**BEGIN**
Step 1: GIVEN: breathing and near-skin vessel displacement I/Q signal sense from 2.4 GHz Doppler radar $x$, for maximum of 60 seconds or time window $t$
Step 2: **for** $x$ and $t$ from 0 to 60, $f'(x_t) \neq f'(x_{t+1})$ do
    **if** $\$result \in \{6, \ldots, 30\}$   // see (3) for $\$result$
    function
    Go to Step 3.
      **if** $\$result \in \{30, \ldots, 80\}$
      Go to Step 4.
        **if** $6 > \$result > 80$
        Go to Step 5.
    **else**
     Go to Step 6.
  **end for**
Step 3: Breathing or pulmonary detected
Step 4: Near-skin vessel or heart-related activities detected
Step 5: Detected object is possibly injured or in an unstable condition with either breathing or heartbeat-related issues.
Step 6: No vital sign signal detected
**END**

- Phase II: From 30 to 60 seconds a) to read pulmonary and vascular signals b) predict the age group of trapped object c) display the estimated distance between the sensor and object d) read the state of health of the object e) determine if the object is non-human (i.e., cat, dog etc.).

Applying the basic geometrical principles of calculus, with reading signal time from 0 to 60 seconds as $x$ and for the entire signal or voltage collected using the Doppler sensor and variation of $x$, $f(x)$, a single inspiration or expiration forms a set of $f'(x) > 0$ as positive or when the object is inhaling. In this case, the distance between the Doppler antennae and the chest wall would be short. $f'(x) = 0$ as stationary points and $f'(x) < 0$ negative or when object exhaling. The first derivative of $f(x)$ or $f'(x) < 0$ or concave downward, shown as Fig. 21, indicates that air is flowing into the lungs from the atmosphere and $f'(x) > 0$ or concave upward, shown as Fig. 22, indicates that airflow from lungs is expelled into the atmosphere.

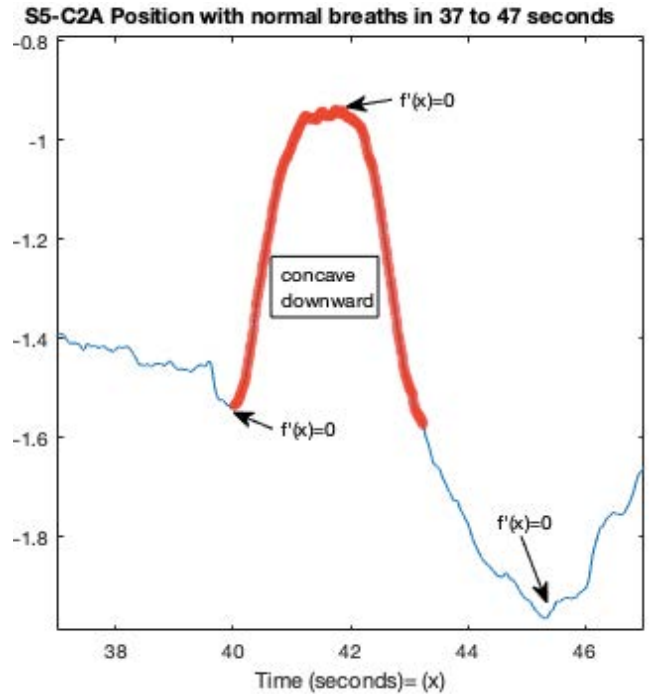Explanations of Table 7. Model-based Anomaly Detection in Time Series



**FIGURE 21.** Inspiration with concave downward and voltage values recorded at f'(x) for stationary would be the smallest.
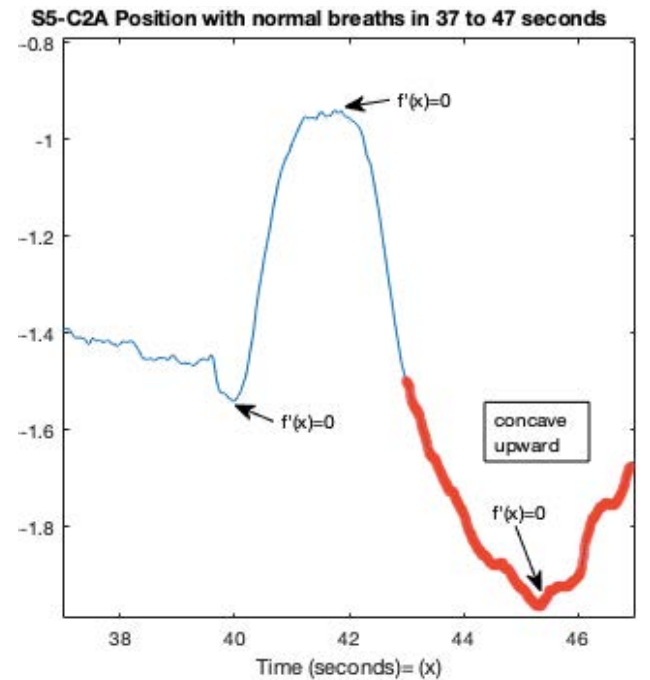


**FIGURE 22.** Expiration with concave upward and voltage values recorded at f'(x) for stationary points would be the biggest.

*Step 1:* Taking in-phase and quadrature (I/Q) continuous wave (CW) Doppler radar at 2.4 GHz signal spectrum for the maximum 60 seconds timeslot per reading [13], [34].
*Step 2:* Using *for* loop to collect the number of times positive and stationary point negative (PSN) or negative and stationary point then positive (NSP) fall within the range

of human breathing and pulse datasets [27], [30], there is a match with human vital signs which potentially indicates whether breathing or pulse related signals are present or no vital signs detected.

*Step 3:* if the reading falls within the range of 6 < $result < 30 in 60 seconds, it indicates there is a possible breathing or pulmonary signal of all ages and an object less than one metre from the sensor according to the empirical laboratory results of this experiment.

*Step 4:* if the reading falls within the range of 6 < $result < 80 in 60 seconds, it indicates a possible near-skin vessel or pulse related signal of all ages has been detected, and the object's position is less than s 0.5 metres from the sensor as per empirical laboratory results for this experiment.

*Step 5:* if the reading falls within the range of 6 > $result > 80 in 60 seconds, that shows there is a possibility the object could be injured or in an unstable condition with either breathing or heartbeat-related issues.

*Step 6:* There is no trace of vital signs from the direction and area in which the Doppler sensor is pointing.

## V. DISCUSSION

With human cardiac activities, a closed blood circulation system requires veins and a capillaries network to carry blood towards the heart and arteries that convey blood away from the heart [24]. With live subjects, blood flow back and forth from and to the heart generates significant movement mainly created by veins, right beneath human skin layers and readable by noncontact sensors [35]. When blood flows from high-pressure areas to regions with lower pressure through a closed vessel network, this displacement activity is measured as 0.2 mm to 0.5 mm around the chest region when the human chest faces directly toward a noncontract sensor antenna [36]. Apart from concentrated research on vessel displacement around the chest region, which has the highest wavelength reading generated from the living subject near-skin vessels, for the neck, arms, and legs shown in Fig. 5 wavelength can also be detected by noncontact sensors in various frequency spectrums [37]–[40].

In this study, we have described and evaluated two methods of noncontact detection of vital signs, particularly breathing and near-skin blood vessel activities. The first method, i.e., the sensor touches the surface of the debris, is used in related research on noncontact vital sign detection; however, the most valuable contribution of this study has been to collect cardiopulmonary datasets whilst, second method, the sensor is not touching the surface of the target of interest. To the best of our knowledge, this method has not been investigated at the time of the paper submission. This method simulates a real disaster event where individuals have just escaped being trapped, maybe hurt themselves, but are desperate to find loved ones. They would be operating the device under solid psychological stress, which may include trembling and shaking. For the result from the first method of data collection, we found the breathing signal can be correctly detected up to

1 meter from the sensor antennae, which reduces to 0.5 meters for near-skin vessel activity.
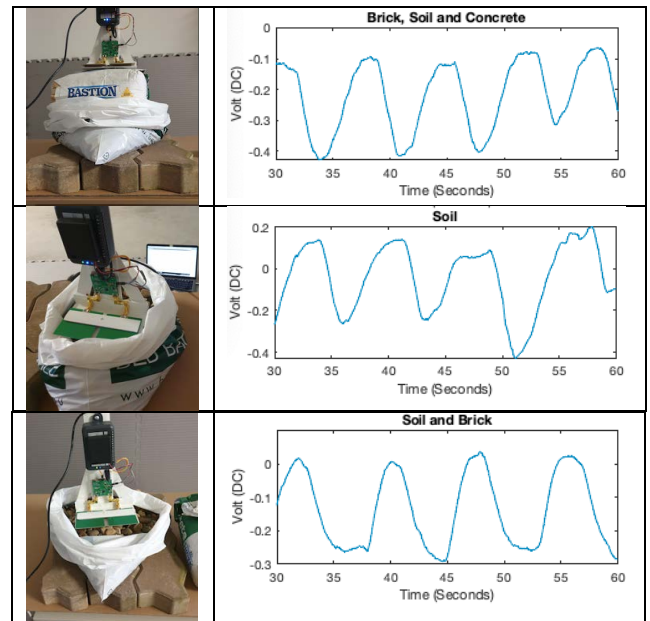


**FIGURE 23.** Breathing results of different sample obstacles collected in 60 seconds.

The paper compared the results of two different data collection methods for impulses from pulmonary and near-skin blood vessels of trapped objects. Regardless of the method used, the accuracy of the breathing-related wave remains at the same level of accuracy. However, with the near-skin blood vessel activity, results are different for different areas of the object's body. See Figs. 12, 13 and 14 for hands or palm for touch-based and Fig. 19 for leg, neck areas for non-touch-based methods. We have conducted and validated pulmonary signal detection through different obstacle materials, and the result (Fig. 23) showed that there is no significant signal output.

## VI. CONCLUSION AND FUTURE WORK

In this paper, we have evaluated a range of obstacle materials between trapped human objects in various positions and the distance to the sensor at which signals can still be read. This empirical research shows pulmonary and near-skin vessel activity readings in relation to the Doppler sensor. Both near-skin vessel and breathing activity can be read when the object is positioned approximately 0.5 metres from the sensor (Fig. 13). In contrast, only pulmonary activities provide readable signals when the object is positioned between 0.5 to 1 meter away from the Doppler sensor. The paper also proposed a theoretical model for a simple anomaly detection algorithm used for time-series applications. It could use a similar approach for empirical data collection to form an anomaly algorithm.

**TABLE 8.** Cardiac and ventilation activities in millimeters [36] contrast with actual Doppler's lambda, and frequency is used.

| Activities | Contraction measured in millimetres (λ) | Contraction estimated in frequency |
|---|---|---|
| Cardiac | 0.2 − 0.5 mm | 1 − 2 (Hz) |
| Ventilation | 4 − 12 mm | 0.1 − 0.3 (Hz) |
| Doppler Sensor operates at 2.4 GHz and 22 MHz channel | 123.67 mm (mean value) | 22 (MHz) |

Future work will include further study of IEEE 802.11b/g/n/ax operated at 2.4 GHz spectrum with 11 channels in day-to-day nonstationary communication devices [41] with evaluation focusing on the wavelength of each spectrum's channel for results from pulmonary and near-skin vessel activities and compare with previous research result from Table. 8. Furthermore, future work may also see the implementation of the pseudo algorithms for active deployment.

## CONFLICT OF INTEREST AND FUNDING

## COMPLIANCE ETHICAL STANDARD

Due to the nature of empirical action research, the methodology would involve a case study, laboratory tests, surveys and readings from humans as the test objects [42]. Thus, ethical issues must be considered carefully. The level of risk to humans from public industrial, scientific and medical (ISM) radio frequency bands [23] which are built into smartphones, would be very slight. With this research method, there is only minimal risk from using computer-type software run in conjunction with the smartphone-liked devices. Nevertheless, the aim of the research is ultimately to involve human subjects during field data collection for heart and breathing rates. Participants in the laboratory environment were volunteers, had read the information sheet and signed the consent form as per the terms and conditions of the ethics approval for this research project, ethic approved protocol number 200201755 from Charles Sturt University, Australia [43]. The participants were aged between 18 and 45 and were in good health at the time of the experiment, showing no signs of illness before or during the vital sign reading sessions.

## ACKNOWLEDGMENT

## REFERENCES

[1] A. G. Macintyre, J. A. Barbera, and E. R. Smith, "Surviving collapsed structure entrapment after earthquakes: A 'time-to-rescue' analysis," *Prehospital Disaster Med.*, vol. 21, no. 1, pp. 4–17, Feb. 2006, doi: 10.1017/s1049023x00003253.

[2] *How Long can Survivors Last Under Rubble?*. BBC. Accessed: Oct. 1, 2020. [Online]. Available: https://www.bbc.com/news/world-32485586

[3] National Review, Inc., "A garment factory in Bangladesh collapsed, killing at least 1, 127 people, with the last survivor rescued after 16 days buried in rubble," *Nat. Rev.*, vol. 65, no. 10, p. 11, 2013.

[4] I. DKL International. *LifeGuard*. Accessed: Jan. 20, 2022. [Online]. Available: http://www.dklabs.com/

[5] R. S. Boyd. *Finding Quake Survivors Just One Use for Remote Heartbeat Detectors*. McClatchy Newspapers. Accessed: Apr. 2, 2021. [Online]. Available: https://www.mcclatchydc.com/news/nation-world/national/article24484201.html

[6] E. Landau. *FINDER Search and Rescue Technology Helped Save Lives in Nepal*. NASA's Jet Propulsion Laboratory, Pasadena, CA, USA. Accessed: Jan. 25, 2021. [Online]. Available: https://www.nasa.gov/jpl/finder-search-and-rescue-technology-helped-save-lives-in-nepal

[7] S. Kara, "Classification of mitral stenosis from Doppler signals using short time Fourier transform and artificial neural networks," *Expert Syst. Appl.*, vol. 33, no. 2, pp. 468–475, Aug. 2007, doi: 10.1016/j.eswa.2006.05.011.

[8] Y. S. Lee, P. N. Pathirana, R. J. Evans, and C. L. Steinfort, "Noncontact detection and analysis of respiratory function using microwave Doppler radar," (in English), *J. Sensors*, vol. 2015, pp. 3–4, Jan. 2015, doi: 10.1155/2015/548136.

[9] P. S. Girão, O. Postolache, G. Postolache, P. M. Ramos, and J. M. D. Pereira, "Microwave Doppler radar in unobtrusive health monitoring," *J. Phys., Conf.*, vol. 588, Feb. 2015, Art. no. 012046, doi: 10.1088/1742-6596/588/1/012046.

[10] A. S. Sovlukov and D. V. Khablov, "The capabilities of microwave methods for alive people detection through obstacles by breathing and heartbeat," *Autom. Remote Control*, vol. 75, no. 11, pp. 2060–2076, Nov. 2014, doi: 10.1134/S0005117914110150.

[11] M. Nosrati and N. Tavassolian, "Effects of antenna characteristics on the performance of heart rate monitoring radar systems," *IEEE Trans. Antennas Propag.*, vol. 65, no. 6, pp. 3296–3301, Jun. 2017, doi: 10.1109/TAP.2017.2694861.

[12] Statista. *Number of Smartphone Users Worldwide From 2016 to 2021*. Accessed: Jan. 30, 2021. [Online]. Available: https://www.statista.com/statistics/330695/number-of-smartphone-users-worldwide/

[13] C. Li, V. M. Lubecke, O. Boric-Lubecke, and J. Lin, "A review on recent advances in Doppler radar sensors for noncontact healthcare monitoring," *IEEE Trans. Microw. Theory Techn.*, vol. 61, no. 5, pp. 2046–2060, May 2013, doi: 10.1109/TMTT.2013.2256924.

[14] Y. J. An, B. H. Kim, G. H. Yun, S. W. Kim, S. B. Hong, and J. G. Yook, "Flexible non-constrained RF wrist pulse detection sensor based on array resonators," *IEEE Trans. Biomed. Circuits Syst.*, vol. 10, no. 2, pp. 8–300, Apr. 2016, doi: 10.1109/TBCAS.2015.2406776.

[15] T. Hall, N. A. Malone, J. Tsay, J. Lopez, T. Nguyen, R. E. Banister, and D. Y. C. Lie, "Long-term vital sign measurement using a non-contact vital sign sensor inside an office cubicle setting," in *Proc. 38th Annu. Int. Conf. IEEE Eng. Med. Biol. Soc. (EMBC)*, Aug. 2016, pp. 4845–4848, doi: 10.1109/EMBC.2016.7591812.

[16] C. C. McGeoch, "Feature article—Toward an experimental method for algorithm simulation," *INFORMS J. Comput.*, vol. 8, no. 1, pp. 1–15, Feb. 1996, doi: 10.1287/ijoc.8.1.1.

[17] S. Ramaswamy, R. Rastogi, and K. Shim, "Efficient algorithms for mining outliers from large data sets," *ACM SIGMOD Rec.*, vol. 29, no. 2, pp. 427–438, May 2000, doi: 10.1145/335191.335437.

[18] C. Gu and C. Li, "Assessment of human respiration patterns via noncontact sensing using Doppler multi-radar system," *Sensors*, vol. 15, no. 3, pp. 6383–6398, 2015, doi: 10.3390/s150306383.

[19] T. Rahman, A. T. Adams, R. V. Ravichandran, M. Zhang, S. N. Patel, J. A. Kientz, and T. Choudhury, "DoppleSleep: A contactless unobtrusive sleep sensing system using short-range Doppler radar," in *Proc. ACM Int. Joint Conf. Pervasive Ubiquitous Comput. (UbiComp)*, Osaka, Japan, 2015, pp. 39–50.

[20] D. N. White, "Johann Christian Doppler and his effect—A brief history," *Ultrasound Med. Biol.*, vol. 8, no. 6, pp. 583–591, 1982, doi: 10.1016/0301-5629(82)90114-4.

[21] K.-M. Chen, Y. Huang, J. Zhang, and A. Norman, "Microwave life-detection systems for searching human subjects under earthquake rubble or behind barrier," *IEEE Trans. Biomed. Eng.*, vol. 47, no. 1, pp. 105–114, Jan. 2000, doi: 10.1109/10.817625.

[22] F. JalaliBidgoli, S. Moghadami, and S. Ardalan, "A compact portable microwave life-detection device for finding survivors," *IEEE Embedded Syst. Lett.*, vol. 8, no. 1, pp. 10–13, Mar. 2016, doi: 10.1109/LES.2015.2489209.

[23] ACMA. *Low Interference Potential Devices (LIPD) Class Licence*. Australian Communications and Media Authority. Accessed: Jan. 27, 2021. [Online]. Available: https://www.acma.gov.au/licences/low-interference-potential-devices-lipd-class-licence

[24] *SEER Training Modules, Cardiovascular System*. U. S. National Institutes of Health, National Cancer Institute. Accessed: Jan. 12, 2020. [Online]. Available: https://training.seer.cancer.gov/anatomy/cardiovascular/

[25] K. Haris, E. Hedström, F. Kording, S. Bidhult, K. Steding-Ehrenborg, C. Ruprecht, E. Heiberg, H. Arheden, and A. H. Aletras, "Free-breathing fetal cardiac MRI with Doppler ultrasound gating, compressed sensing, and motion compensation," *J. Magn. Reson. Imag.*, vol. 51, no. 1, pp. 260–272, Jan. 2020, doi: 10.1002/jmri.26842.

[26] C. C. Huang, P. Y. Lee, P. Y. Chen, and T. Y. Liu, "Design and implementation of a smartphone-based portable ultrasound pulsed-wave Doppler device for blood flow measurement," *IEEE Trans. Ultrason., Ferroelectr., Frequency Control*, vol. 59, no. 1, pp. 8–182, Jan. 2012, doi: 10.1109/TUFFC.2012.2171.

[27] J. Crisp, *Potter & Perry's Fundamentals of nursing* (Potter and Perry's Fundamentals of nursing), 4th ed. Chatswood, NSW, Australia: Elsevier, 2012.

[28] M. A. Oyama, M. S. Kraus, and A. R. Gelzer, *ECG Interpretation in Small Animal Practice (Rapid Review)*. Boca Raton, FL, USA: CRC Press, 2014.

[29] D. C. Silverstein and K. Hopper, *Small Animal Critical Care Medicine*, 2nd ed. Saint Louis, MO, USA: Elsevier, 2015.

[30] W. Q. Lindh, M. Pooler, C. D. Tamparo, and B. M. Dahl, *Delmar's Comprehensive Medical Assisting: Administrative and Clinical Competencies* (Delmar's Comprehensive Medical Assisting), 4th ed. Boston, MA, USA: Cengage Learning, 2009, p. 1552.

[31] A. De Leo, V. Petrini, P. Russo, L. Scalise, V. Di Mattia, V. M. Primiani, and G. Cerri, "An EM modeling for rescue system design of buried people," *Int. J. Antennas Propag.*, vol. 2015, pp. 1–7, 2015, doi: 10.1155/2015/465651.

[32] M. Elstad, E. L. O'Callaghan, A. J. Smith, A. Ben-Tal, and R. Ramchandra, "Cardiorespiratory interactions in humans and animals: Rhythms for life," *Amer. J. Physiol. Heart Circulatory Physiol.*, vol. 315, no. 1, pp. H6–H17, Jul. 2018, doi: 10.1152/ajpheart.00701.2017.

[33] P. Wang, Y. Ma, F. Liang, Y. Zhang, X. Yu, Z. Li, Q. An, H. Lv, and J. Wang, "Non-contact vital signs monitoring of dog and cat using a UWB radar," *Animals*, vol. 10, no. 2, p. 205, Jan. 2020, doi: 10.3390/ani10020205.

[34] V. L. Petrović, M. M. Janković, A. V. Lupšić, V. R. Mihajlović, and J. S. Popović-Boövović, "High-accuracy real-time monitoring of heart rate variability using 24 GHz continuous-wave Doppler radar," *IEEE Access*, vol. 7, pp. 74721–74733, 2019, doi: 10.1109/ACCESS.2019.2921240.

[35] J. Kranjec, S. Beguš, G. Geršak, and J. Drnovšek, "Non-contact heart rate and heart rate variability measurements: A review," *Biomed. Signal Process. Control*, vol. 13, pp. 102–112, Sep. 2014, doi: 10.1016/j.bspc.2014.03.004.

[36] D. Obeid, S. Sadek, G. Zaharia, and G. E. Zein, "Multitunable microwave system for touchless heartbeat detection and heart rate variability extraction," *Microw. Opt. Technol. Lett.*, vol. 52, no. 1, pp. 192–198, Jan. 2010, doi: 10.1002/mop.24877.

[37] J.-C. Liou, Y.-C. Hsiao, and C.-F. Yang, "Infrared sensor detection and actuator treatment applied during hemodialysis," *Sensors*, vol. 20, no. 9, p. 2521, Apr. 2020, doi: 10.3390/s20092521.

[38] E. J. Sirevaag, S. Casaccia, E. A. Richter, J. A. O'Sullivan, L. Scalise, and J. W. Rohrbaugh, "Cardiorespiratory interactions: Noncontact assessment using laser Doppler vibrometry," *Psychophysiology*, vol. 53, no. 6, pp. 847–867, 2016, doi: 10.1111/psyp.12638.

[39] H. M. Stauss, E. A. Anderson, W. G. Haynes, and K. C. Kregel, "Frequency response characteristics of sympathetically mediated vasomotor waves in humans," *Amer. J. Physiol. Heart Circulatory Physiol.*, vol. 274, no. 4, pp. H1277–H1283, Apr. 1998, doi: 10.1152/ajpheart.1998.274.4.H1277.

[40] V. V. Zaytsev, S. V. Miridonov, O. V. Mamontov, and A. A. Kamshilin, "Contactless monitoring of the blood-flow changes in upper limbs," *Biomed. Opt. Exp.*, vol. 9, no. 11, pp. 5387–5399, Nov. 2018, doi: 10.1364/BOE.9.005387.

[41] D.-J. Deng, Y.-P. Lin, X. Yang, J. Zhu, Y.-B. Li, J. Luo, and K.-C. Chen, "IEEE 802.11ax: Highly efficient WLANs for intelligent information infrastructure," *IEEE Commun. Mag.*, vol. 55, no. 12, pp. 52–59, Dec. 2017, doi: 10.1109/MCOM.2017.1700285.

[42] M. D. Myers, *Qualitative Research in Business & Management*, 2nd ed. London, U.K.: Sage, 2013.

[43] CSU. *Research Integrity, Ethics and Compliance*. Charles Sturt University. Accessed: Feb. 1, 2021. [Online]. Available: https://research.csu.edu.au/integrity-ethics-compliance

**LINH PHAM** (Member, IEEE) received the Master of Networking and Systems Administration degree from Charles Sturt University, Australia, in 2004. From 2004 to 2021, he was an Adjunct Lecturer with Charles Sturt University–Sydney Study Centres. He has published 13 conference papers and contains two best paper awards on this very research topics, nine journals and one special issue with IEEE conferences and Elsevier journals. His research interest includes noncontact detecting and identify human entrapment's cardiopulmonary vital signs using a 2.4 GHz radio frequency spectrum.

**MANORANJAN PAUL** (Senior Member, IEEE) received the Ph.D. degree from Monash University, Melbourne, VIC, Australia, in 2005. He was a Postdoctoral Research Fellow with the University of New South Wales, Monash University, and Nanyang Technological University. He is currently a Professor and the Director of the Computer Vision Laboratory, and the Leader of the Machine Vision and Digital Health Research Group, Charles Sturt University (CSU), Bathurst, NSW, Australia. He has authored or coauthored more than 168 refereed publications, including 60 journals. His major research interests include video analytics, E-health, wine technology, and imaging/signal processing. He was a recipient of the ICT Researcher of the Year 2017 awarded by the Australian Computer Society. He was a General Co-Chair of PSIVT 2019 and a Program Co-Chair of PSIVT 2017 and DICTA 2018. He is an Associate Editor of the IEEE TRANSACTIONS ON CIRCUITS AND SYSTEMS FOR VIDEO TECHNOLOGY, IEEE TRANSACTIONS ON MULTIMEDIA, and *EURASIP Journal in Advances on Signal Processing*. He has conducted invited keynote speeches in IEEE DICTA 2017 and 2013, WoWMoM 2014, and ICCIT 2010. He obtained more than $4.2 m competitive external grant, including two Australian Research Council (ARC) Discovery Project Grants. He has supervised 15 Ph.D. students to completion.

**PWC PRASAD** (Senior Member, IEEE) received the bachelor's and master's degrees from Saint Petersburg Electrotechnical University and the Ph.D. degree from Multimedia University, Malaysia. He is currently an Associate Professor with the School of Computing and Mathematics, Charles Sturt University, Australia. Prior to this, he was a Lecturer at United Arab Emirates University, UAE; Multimedia University, Malaysia; and the Informatics Institute of Technology (IIT), Sri Lanka. He is an active researcher in the areas of computer architecture, digital systems, and modeling and simulation. He has published more than 250 research articles in computing and engineering journals and conferences proceedings. He has coauthored two books titled *Digital Systems Fundamentals* and *Computer Systems Organization and Architecture* (Prentice Hall). He is a Senior Member of the IEEE Computer Society.

● ● ●